

Response of the South Atlantic circulation to an abrupt Atlantic THC collapse

Audine Laurian and Sybren S. Drijfhout

Royal Netherlands Meteorological Institute, De Bilt, the Netherlands

Submitted to *Climate Dynamics*

December 28th, 2009

Corresponding author: Sybren S. Drijfhout, email: drijfhout@knmi.nl

Abstract

The South Atlantic response to a North Atlantic thermohaline circulation (THC) collapse is investigated in the ECHAM5/MPI-OM climate model. A slightly reduced Agulhas leakage (about 2.2 Sv; $1 \text{ Sv} = 10^6 \text{ m}^3 \cdot \text{s}^{-1}$) is found to be associated with a somewhat weaker Southern Hemisphere (SH) supergyre and Indonesian throughflow (ITF). These changes are due to reduced wind stress curl over the SH supergyre, associated with a weaker Hadley circulation and a weaker SH subtropical jet. The northward cross-equatorial transport of thermocline and intermediate waters is much more strongly reduced in relation with a THC collapse. A cross-equatorial gyre develops due to an anomalous wind stress curl over the tropics that results from the anomalous SST gradient associated with reduced ocean heat transport. This cross-equatorial gyre completely blocks the transport of thermocline waters from the South to the North Atlantic. The waters originating from Agulhas leakage flow somewhat deeper and most of it recirculates in the South Atlantic subtropical gyre, leading to a gyre intensification. This intensification is consistent with the anomalous surface cooling over the South Atlantic. Most changes in South Atlantic circulation due to global warming, featuring a reduced THC, are qualitatively similar to the response to a THC collapse, but smaller in amplitude. However, the increased northward cross-equatorial transport of intermediate water relative to thermocline water is a strong fingerprint of a THC collapse.

1. Introduction

The stability characteristics of the THC for the 21st century are not well known (*Weber et al. 2007; Yin and Stouffer 2007*). The THC might weaken by 25 (± 25)% until 2100 due to global warming (*Schmittner et al. 2005*), but the weakening induced by anthropogenic forcing may as well remain within the range of natural variability during the next several decades (*Latif et al. 2006*).

On the other hand, in response to freshwater forcing, the THC features a hysteresis response which depends on the precise oceanic conditions (*Rahmstorf et al. 2005; Huisman et al. 2009*). When the

THC resides in the multiple equilibria regime, a freshwater pulse may lead to a collapse which has global impacts (*Vellinga and Wood 2002; Drijfhout 2009*). A strong sea surface temperature (SST)-driven cooling of the Northern Hemisphere (NH) leads to a reduced (respectively increased) poleward oceanic (resp. atmospheric) heat transport, which in turn leads to a weak warming of the South Atlantic, associated with a reversed North Brazil Current (NBC; *Dong and Sutton 2002; Cheng et al. 2007; Chang et al. 2008*).

In the South Atlantic, the upper limb of the THC is primarily made of Agulhas leakage which connects the Indian and the Atlantic Oceans (*Gordon 1985; de Ruijter et al. 1999; Richardson 2007*). Agulhas rings cross the South Atlantic along dominantly westward tracks (*Schouten et al. 2000*), but the majority of their water mass is mixed with the surrounding due to multiple splitting and merging events (*Boebel et al. 2003; de Steur et al. 2004*). This water then flows with the Benguela Current (BeC), which is the main conduit for the upper branch of the THC in the eastern South Atlantic (*Garzoli and Gordon 1996; Drijfhout et al. 2003*). Off the coast of Brazil, the BeC splits into the NBC which flows equatorward, and the Brazil Current (BrC) which recirculates in the subtropical gyre via the South Atlantic Current (SAC; *Stramma and England 1999*). The SAC eventually feeds the Indian and Pacific Oceans to form the so-called “supergyre” (*Ridgway and Dunn 2007; Speich et al. 2007*). Changes in Agulhas leakage are associated with changes in the THC. Buoyancy anomalies associated with variations in Agulhas leakage impact the meridional overturning circulation (MOC) over the whole South Atlantic (*Biastoch et al. 2008*) and ultimately influence deep water formation in the North Atlantic (*Weijer et al. 2002*).

The response of the South Atlantic to a THC collapse may either feature a cessation of Agulhas leakage or a stronger recirculation in the South Atlantic subtropical gyre and in the supergyre of the waters originating from Agulhas leakage. If so, the waters originating from Agulhas leakage would no longer feed the NBC but the BrC and SAC instead. The aim of this study is to investigate how the South

Atlantic circulation reorganizes in response to a North Atlantic THC collapse. In Section 2, the ECHAM5/MPI-OM climate model and the water-hosing experiment are presented, and the model is validated against observations. Changes in South Atlantic circulation due to a THC collapse are presented in Section 3. The change in Agulhas leakage and the fate in the South Atlantic of the waters originating from the anomalous leakage are assessed in Section 4. In Section 5, the changes in the South Atlantic are linked to the anomalous surface forcing. In Section 6, the response in the South Atlantic to a THC collapse is compared to the global warming signal which features a weakened THC. The results are summarized in Section 7.

2. Model, hosing experiment, and validation against observations

2.1. Model and water-hosing experiment

The results of this study are obtained with the ECHAM5/MPI-OM climate model (*Roeckner et al. 2003; Marsland et al. 2003*). The ocean model has a horizontal resolution of about 1.4° by 1.4° away from the poles, it is highest near the poles ($O(20-40\text{ km})$), and the meridional resolution is refined near the equator to 0.5° . It has 40 vertical levels. The atmospheric model has 31 vertical levels and a horizontal resolution of T63. A 17-member ensemble of model simulations was performed over the period 1950-2100 as part of the ESSENCE project (*Sterl et al. 2008*). From 1950 to 2000 the simulations were forced by the observed concentrations of greenhouse gases (GHG) and tropospheric sulfate aerosols. From 2001 to 2100 the simulations followed the SRES A1b scenario (*Intergovernmental Panel on Climate Change 2000*). Each simulation was initialized from a single long simulation in which historical GHG concentrations have been used until 1950. Here, two 5-member ensemble simulations are compared. One 5-member ensemble is a subset of the 17-member baseline experiment and is the reference ensemble. In the second 5-member ensemble, a freshwater anomaly of 1 Sv was uniformly applied over the northern North Atlantic Ocean between 50°N and 70°N from 2001 onwards, starting

from the five initial states of the first ensemble. This freshwater supply leads to an abrupt reduction of the THC within 20 years from about 20 to 6 Sv (Fig. 1). After the collapse, an almost stationary anomaly pattern prevails which can be seen as the fingerprint of the THC collapse on the atmosphere (*Laurian et al.* 2009a). In the other ensemble the THC gradually weakens by 20% after 100 years due to global warming. The response to a THC collapse is addressed by comparing the ensemble mean of the perturbed simulations over the period 2081-2100 (named HO), to that of the associated control simulations over the same period (called E2). The response to global warming is addressed by comparing E2 to the ensemble mean of the control simulations over the period 1981-2000 (named E1).

In the real world, Agulhas leakage is largely achieved by the intermittent shedding of eddies, and to a much lesser extent by a continuous flow at the inshore side of the Agulhas Current (*de Ruijter et al.* 1999). In the coarse resolution model, Agulhas leakage solely consists of a viscosity-driven continuous flow into the South Atlantic that branches off the Agulhas Current where it retroflects.

The response of the South Atlantic circulation to a THC collapse is diagnosed by calculating mass transports in neutral density layers. We define four density classes using the neutral density as vertical coordinate (*Jackett and McDougall* 1997): surface/thermocline waters (noted S) whose densities are lighter than $1025.5 \text{ kg} \cdot \text{m}^{-3}$; intermediate waters (noted I) with densities heavier than $1025.5 \text{ kg} \cdot \text{m}^{-3}$ and lighter than $1027 \text{ kg} \cdot \text{m}^{-3}$; deep waters (noted D) with densities heavier than $1027 \text{ kg} \cdot \text{m}^{-3}$ and lighter than $1027.8 \text{ kg} \cdot \text{m}^{-3}$; and bottom waters (noted B) with densities heavier than $1027.8 \text{ kg} \cdot \text{m}^{-3}$.

2.2. Model validation against observations

In the modeled circulation of the South Atlantic, the water pathways in the upper limb of the THC are in agreement with the pathways depicted by *Stramma and England* (1999). Thermocline waters enter the South Atlantic via Agulhas leakage and flow equatorward in the BeC and the NBC (Fig. 2a). Intermediate waters also flow in the BeC. Part of them follow the equatorward route as for the

thermocline waters, the rest flows southward in the BrC and feeds the SAC (Fig. 2b).

The zonally integrated mass transport in the Atlantic at 32°S is compared to observations from *Ganachaud and Wunsch* (2000; noted GW00) and *Sloyan and Rintoul* (2001; noted SR01) (Fig. 3). Note that GW00 considered three ocean layers with merged thermocline and intermediate waters. To compare the model to their observations, we assigned half of their upper layer transport value to the thermocline layer and the other half to the intermediate layer. At 32°S, the modeled overturning is slightly stronger than in the observations. About 18.8 Sv of surface and intermediate waters flow northward compared to 16 Sv in GW00 and 10 Sv in SR01. This upper limb of the THC is mainly compensated by the southward transport of NADW on the order of 22.5 Sv in the model (23 Sv in GW00 and 17 Sv in SR01). About 4 Sv of Antarctic Bottom Waters (AABW) flows northward in the model, which agrees with the 6 Sv observed by GW00 and SR01. We infer from this comparison that the model is able to reproduce the mean characteristics of the South Atlantic circulation.

3. Response of the South Atlantic circulation to a THC collapse

In response to a THC collapse, the barotropic circulation features a reduced Agulhas Current and reduced Agulhas leakage, as well as a reduced supergyre (Fig. 4). This suggests that the anti-correlation between the strength of the Agulhas Current and that of Agulhas leakage, as found by *van Sebille et al.* (2009), does not hold for circulation changes driven by very large freshwater perturbations. This comes as no surprise as the relation of *van Sebille et al.* (2009) was a linearization around present-day climate, with most variations in Agulhas leakage caused by winds. On the other hand, the SAC and the ACC are enhanced in response to a THC collapse (Fig. 4).

Also, the northward flow in the South Atlantic is changed, in particular in the thermocline and intermediate layers (Fig. 5). The cross-equatorial transport is strongly reduced in the thermocline in agreement with *Chang et al.* (2008). The subtropical gyre is intensified and the southward transport by

the BrC is enhanced. These changes are in agreement with model results for the LGM period (*Clauzet et al. 2007*). Changes in deep and bottom flows are small (not shown).

In agreement with the changes in northward flow in the South Atlantic upper layers, the zonally integrated mass transport at 32°S features an 8.7 Sv decrease in northward transport, with a southward transport in the thermocline of 2.3 Sv and a northward transport in the intermediate layer of 7.9 Sv (Fig. 6a). The NADW transport is reduced from 17 to 7 Sv due to the freshwater input in the northern North Atlantic (in agreement with Fig. 1). The northward transport of AABW is slightly reduced and the overturning circulation at 32°S is weakened in response to a THC collapse. The fate of the northward mass transport in the intermediate layer at 32°S is illustrated by the zonally integrated mass transport at 25°N in the Atlantic (Fig. 6b). There, there is no northward transport in the thermocline, and the northward transport in the intermediate layer is slightly enhanced by 0.2 Sv from 4.2 to 4.4 Sv. This means that the cross-equatorial transport in the intermediate layer is less than its value at 32°S. The South Atlantic features a shallow reversed overturning cell. The NADW transport at 25°N is also reduced by about 10.8 Sv, the bottom water transport is not significantly changed. These changes are consistent with the changes in MOC (not shown) and the change in maximum MOC value displayed in Fig. 1.

4. Tracking the changes of waters originating from Agulhas leakage

A set of zonal and meridional sections were defined, across which the changes in mass transports are analyzed (Fig. 2a). Changes in Agulhas leakage proper due to a THC collapse have been assessed by analyzing the change in zonal mass transport at 23°E between 30-40°S. The fate of the waters originating from Agulhas leakage is investigated by analyzing the cross-equatorial transport in the NBC at 2°S between 40-30°W, and by analyzing the recirculation in the BrC at 40°S, between 70-40°W.

4.1. Change in Agulhas leakage

During the last two decades of the 21st century, the modeled Agulhas leakage is on the order of 17.2 Sv. Fig. 7 shows a reduced Agulhas leakage by 2.2 Sv in response to a THC collapse. This implies that the response of Agulhas leakage to a THC collapse is small compared to the reduction in NADW transport (from 17 to 7 Sv at 32°S; Fig. 6a), and compared to the reduction in northward transport at 25°N (from 14.9 to 4.4 Sv; Fig. 6b). More than 89% of the total transport in Agulhas leakage takes place in the thermocline and intermediate layers. In response to a THC collapse, the transport in Agulhas leakage of thermocline and intermediate waters is reduced by 1.8 Sv and by 1.1 Sv respectively. This suggests that about 7.6 Sv of waters originating from Agulhas leakage stays in the South Atlantic and participates in an increased subtropical gyre recirculation. Most reduction in Agulhas leakage is associated with reduced recirculation in the greater Agulhas system and in the southeast Atlantic (Fig. 4). The whole supergyre has become slightly weaker, as well as the transport in the ITF (decreased by about 1.9 Sv; not shown). The southern edge of the supergyre, the SAC, however, is enhanced. Overall, the supergyre has become weaker but the South Atlantic recirculation has become stronger.

4.2. Response of the subtropical gyre recirculation

Part of the remaining waters that originate from Agulhas leakage are transported in the BeC towards the BrC. In response to a THC collapse, more thermocline and intermediate waters are transported southward. Fig. 8 shows the zonally integrated layer mass transport at 40°S between 70-40°W in the BrC. This section is located just north of the Falkland Current retroflection, which provides cold waters from Drake Passage to the South Atlantic (*Stramma and England 1999*). The subtropical gyre recirculation is enhanced by about 8.9 Sv in response to a THC collapse. The DWBC however, is reduced by 6.1 Sv, which is consistent with the previous discussion.

4.3. Response of the cross-equatorial transport

In response to a THC collapse, less thermocline water is transported by the BeC across 10°W (8.6 Sv in HO; 12.1 Sv in E2; not shown) consistent with Fig. 5a. In the thermocline and intermediate layers, the equatorward transport is reduced by only 1.5 Sv, consistent with enhanced recirculation of these waters in the South Atlantic. The cross-equatorial transport achieved by the NBC (about 22.4 Sv in E2) is reduced by up to 12.7 Sv in response to a THC collapse (Fig. 9; in agreement with *Chang et al. 2008*). The DWBC (17.7 Sv in E2) is also reduced by about 11.3 Sv in response to a THC collapse. These transports are still much higher than the collapsed North Atlantic THC would suggest. To further investigate the fate of the northward transport of thermocline and intermediate waters within the NBC, the zonally integrated meridional transport across 2°S as a function of longitude is shown in Fig. 10. The decreased northward transport in the thermocline (Fig. 9) is highlighted by Fig. 10a. Although this transport is northward between the Brazilian coast and about 5°W , it is overall southward (on the order of 2 Sv) at 2°S . This indicates that part of the cross-equatorial flow in the thermocline recirculates in the Tropical Atlantic (see Fig. 4). This recirculation corresponds to the existence of a cross-equatorial gyre within the upper layers of the tropical Atlantic (*Lee and Wang 2008*). Such a gyre develops because of the reduced ocean heat transport due to a THC collapse (*Laurian et al. 2009a*). As a result, an anomalous cross-equatorial SST gradient develops (*Drijfhout 2009*) that induces cross-equatorial winds which are reinforced by a wind-evaporation-SST (WES) feedback. The anomalous wind stress curl develops the cross-equatorial gyre which only affects the transport of thermocline waters. Below the thermocline the northward transport of intermediate waters is slightly increased (on the order of 6 Sv; Fig. 10b). This small increase (on the order of 1 Sv) is due to the slight densification of the waters originating from Agulhas leakage due to a THC collapse. The deep waters are transported southward and this transport is strongly reduced due to a THC collapse (7 Sv v.s. 17 Sv as shown previously; Fig. 10c).

5. Water mass transformation in the Agulhas retroflection area

The gyre circulation is driven by buoyancy and steered by the wind (*Luyten and Stommel 1986; Cushman-Roisin 1987*). In the South Atlantic, the mean net buoyancy flux (*Marshall et al. 1993; Downes et al. 2009*) is dominated by the surface heatflux (Fig. 11a). There, the strongest signals are the heat loss over Agulhas leakage (on the order of $210 \text{ W} \cdot \text{m}^{-2}$), and the heat loss at 40°S , just north of the Falkland Current retroflection. In response to a THC collapse, changes in buoyancy and wind are primarily ocean-driven because the large freshwater perturbation in the northern North Atlantic first affects the SST which then drives the atmospheric temperature response (*Cheng et al. 2007; Laurian et al. 2009b*). In the North Atlantic, the cooler ocean cools the atmosphere and in the SH the warmer ocean warms the atmosphere (Fig. 11b; see *Laurian et al. 2009b*). In the South Atlantic, the strongest responses are a heat loss by the ocean to the atmosphere in the Benguela upwelling region of about $100 \text{ W} \cdot \text{m}^{-2}$, and a heat gain by the ocean in the Agulhas retroflection area of about $70 \text{ W} \cdot \text{m}^{-2}$. But, in most part of the South Atlantic, the anomalous air-sea heatflux due to a THC collapse is heat loss cooling the ocean. This anomalous cooling acts to intensify the South Atlantic subtropical gyre (*Cushman-Roisin 1987*). Outside the South Atlantic, the cooling signal is much weaker, and in particular over the supergyre where the reduced wind stress curl dominates the gyre response.

In response to a THC collapse, the winds and associated wind stress in the SH change (*Cheng et al. 2007*) and modify the Ekman pumping. The southern South Atlantic is characterized by enhanced downwelling (reduced upwelling); in the Agulhas retroflection the opposite response is seen (Fig. 12). The BeC is characterized by upwelling which is reduced due to the THC collapse (in agreement with *Haarsma et al. 2008*). The wind stress curl is overall reduced in the supergyre, upstream of Agulhas leakage, and it is increased downstream of Agulhas leakage (Fig. 12). The slight reduction in Agulhas leakage is thus due to the reduced supergyre circulation (Fig. 4) rather than caused by a latitudinal shift in the subtropical front as suggested by paleo studies (*Bard and Rickaby 2009*). The increased wind stress

curl downstream of Agulhas leakage contributes to a denser flow there, hence a stronger transport in the intermediate layer. This Ekman pumping response also leads to an enhanced recirculation in the South Atlantic subtropical gyre, while the supergyre as a whole is weakened. This signal is consistent with increased recirculation of waters originating from Agulhas leakage in the South Atlantic, while Agulhas leakage itself is decreased. The weaker supergyre can be explained by decreased westerlies in the SH. *Drijfhout* (2009) shows that the THC collapse is associated with a southward shift of the rising branch of the atmospheric mean meridional circulation, similar as in Austral summer. This implies a weaker SH Hadley cell, and a decreased subtropical jet there. The signal of reduced westerlies in the SH extends all the way to the surface between 30°S and 50°S. As a result, the supergyre weakens.

6. Comparison between the response to a THC collapse and that to global warming

Because global warming features a reduced THC, qualitatively similar to the response to freshwater hosing, we compare the response in HO-E2 to that in E2-E1. In response to global warming, Agulhas leakage reduces, mainly in the intermediate layer (not shown). This reduction is weaker than that due to a THC collapse and is likewise associated with a reduced supergyre circulation. Both the SH Hadley cell and the subtropical jet weaken in response to global warming. But contrary to the case of a THC collapse where the NH Hadley cell and subtropical jet strengthen (*Drijfhout* 2009), the NH and SH responses to global warming are similar. The northward cross-equatorial transport reduction is now mainly occurring in the intermediate layer (Fig. 13); the MOC not only weakens but also shoals, and the South Atlantic does not feature heat loss, but heat gain, as for global warming the driver of the climate change resides in the atmosphere, while in case of a THC collapse it is due to the ocean. The shift to lower density classes in the upper branch of the northward flow across 32°S was also found by *Downes et al.* (2009). The increased northward transport of intermediate waters at 2°S in the water-hosing experiment (Fig. 9) is therefore a strong fingerprint of THC collapse. In response to global warming, the

South Atlantic subtropical gyre intensifies as well; the reduction in cross-equatorial transport of thermocline and intermediate waters is also in this case larger than the reduction in Agulhas leakage. *Biastoch et al. (2009)* report an increase in Agulhas leakage due to a poleward shift of SH westerlies. In the global warming run, the decrease in SH westerlies is a more robust signal than its poleward shift, and Agulhas leakage subsequently reduces. Part of the explanation might be that the shift in SH westerlies is largely driven by anthropogenic ozone changes (*Son et al. 2009*). Also, because in the model Agulhas leakage does not occur via ring shedding, but via the viscosity driven coastal current, the response of leakage to meridional shifts in the wind might be different than when leakage predominantly occurs via the formation of Agulhas rings.

7. Summary and conclusions

The response of the South Atlantic circulation to a THC collapse was investigated in the ECHAM5/MPI-OM climate model. A slightly reduced Agulhas leakage (2.2 Sv) was found to be associated with a somewhat weaker supergyre and a weaker ITF. These changes are due to reduced wind stress over the supergyre, associated with a weaker Hadley circulation and an anomalous tropical SST that mimics Austral summer. The northward cross-equatorial transport is much more strongly reduced in response to a collapse of the THC. In the tropics, a cross-equatorial gyre develops associated with reduced ocean heat transport, anomalous SST gradient and anomalous wind stress curl reinforced by a WES feedback. The remaining net cross-equatorial transport solely consists of intermediate water. The waters originating from Agulhas leakage start flowing deeper, and flow more within the intermediate layer, due to enhanced cooling and downwelling in the South Atlantic. They more often recirculate in the South Atlantic subtropical gyre, leading to an intensified gyre there. The changes in South Atlantic circulation due to a THC collapse are much stronger than the response to global warming, but in many respects qualitatively similar. However, increased northward cross-equatorial transport of intermediate

water relative to the transport of thermocline water is a fingerprint of the THC collapse, while the response to global warming features the opposite behavior.

Acknowledgments

This work was granted by the Dutch Ministry of Transport, Public Works and Water Management. The ESSENCE project, lead by Wilco Hazeleger (KNMI) and Henk Dijkstra (UU/IMAU), was carried out with support of DEISA, HLRS, SARA, and NCF (through NCF projects NRG-2006.06, CAVE-60-023 and SG-06-267). We thank the DEISA Consortium (co-funded by the EU, FP6 projects 508830/031513) for support within the DEISA Extreme Computing Initiative (www.deisa.org). The authors thank Andreas Sterl and Camiel Severijns (KNMI), and HLRS and SARA staff for technical support. We greatly appreciated the discussions with B. Sloyan and J. Mignot.

Bibliography

- Bard E, and Rickaby REM (2009) Migration of the subtropical front as a modulator of glacial climate, *Nature*, 460, 380-384
- Biastoch A, Böning CW, and Lutjeharms JRE (2008) Agulhas leakage dynamics affects decadal variability in Atlantic overturning circulation, *Nature*, 456, 489-492
- Biastoch A, Böning CW, Schwarzkopf FU, and Lutjeharms JRE (2009) Increase in Agulhas leakage due to poleward shift of Southern Hemisphere westerlies, *Nature*, 462, 495-499
- Boebel O, Lutjeharms JRE, Schmid C, Zenk W, Rossby T, and Barron CN (2003) The Cape Cauldron, a regime of turbulent inter-ocean exchange, *Deep Sea Res.*, 50, 57-86
- Chang P, Zhang R, Hazeleger W, Wen C, Wan X, Ji L, Haarsma RJ, Breugem WP, and Seidel H (2008) Oceanic link between abrupt changes in the North Atlantic Ocean and the African monsoon, *Nature Geosciences*, 1, 444-448
- Cheng W, Bitz CM, and Chiang JCH (2007) Adjustment of the Global Climate to an Abrupt Slowdown of the Atlantic Meridional Overturning Circulation, *Geophys. Monogr.* 1973, 295-314
- Clauzet G, Wainer I, Lazar A, Brady E, and Otto-Bliesner B (2007) A numerical study of the South Atlantic circulation at the Last Glacial Maximum, *Palaeogeogr. Palaeoclim. Palaeoeco.*, 253, 509-528
- Cushman-Roisin B (1987) On the Role of Heat Flux in the Gulf Stream-Sargasso Sea Subtropical Gyre System, *J. Phys. Oceanogr.*, 17, 2189-2202
- de Ruijter WPM, Biastoch A, Drijfhout SS, Lutjeharms JRE, Matano RP, Pichevin T, van Leeuwen PJ, and Weijer W (1999) Indian-Atlantic interocean exchange: Dynamics, estimation and impact, *J. Geophys. Res.*, 104, 20,885-20,910
- de Steur L, van Leeuwen PJ, and Drijfhout SS (2004) Tracer leakage from modeled Agulhas Rings, *J. Phys. Oceanogr.*, 34, 1387-1399

- Dong BW, and Sutton RT (2002) Adjustment of the coupled ocean–atmosphere system to a sudden change in the Thermohaline Circulation, *Geophys. Res. Lett.*, 29, doi:10.1029/2002GL015229.
- Downes SM, Bindoff NL, and Rintoul SR (2009) Impacts of Climate Change on the Subduction of Mode and Intermediate Water Masses in the Southern Ocean, *J. Clim.*, 22, 3289-3302
- Drijfhout SS, de Vries P, Döös K, and Coward AC (2003) Impact of eddy-induced transport on the Lagrangian structure of the upper branch of the Thermohaline Circulation, *J. Phys. Oceanogr.*, 33, 2141-2155
- Drijfhout SS (2009) The atmospheric response to a THC collapse: Scaling relations for the Hadley circulation and the nonlinear response in a coupled climate model, *J. Clim.*, doi:10.1175/2009JCLI3159.1
- Ganachaud A, and Wunsch C (2000) Improved estimates of global ocean circulation, heat transport and mixing from hydrographic data, *Nature*, 408, 453-456
- Garzoli SL, and Gordon AL (1996) Origins and variability of the Benguela Current, *J. Geophys. Res.*, 101, 897-906
- Gordon AL (1985) Indian-Atlantic Transfer of Thermocline Water at the Agulhas Retroflection, *Science*, 227, 1030-1033
- Haarsma RJ, Campos E, Hazeleger W, and Severijns C (2008) Influence of the Meridional Overturning Circulation on Tropical Atlantic Climate and Variability, *J. Clim.*, 21, 1403-1416
- Huisman SE, den Toom M, Dijkstra HA, and Drijfhout SS (2009) An indicator of the multiple equilibria regime of the Atlantic Meridional Overturning Circulation, *J. Phys. Oceanogr.*, doi:10.1175/2009JPO4215.1
- Intergovernmental Panel on Climate Change (2000) Special Report on Emissions Scenarios : a special report of Working Group III of the Intergovernmental Panel on Climate Change, edited by N.

Nakicenovic et al., Cambridge University Press, New York

Jackett DR, and TJ McDougall (1997) A Neutral Density Variable for the World's Oceans, *J. Phys. Oceanogr.*, 27, 237-263

Latif M, Böning C, Willebrand J, Biastoch A, Dengg J, Keenlyside N, Schweckendiek U, and Madec G (2006) Is the Thermohaline Circulation Changing?, *J. Clim.*, 19, 4631–4637

Laurian A, Drijfhout SS, Hazeleger W, and van Dorland R (2009a) Global surface cooling: The atmospheric fast feedback response to a collapse of the thermohaline circulation, *Geophys. Res. Lett.*, 36, doi:10.1029/2009GL040938

Laurian, A, SS Drijfhout, W Hazeleger, and B van den Hurk (2009b) Response of the Western European climate to a collapse of the thermohaline circulation, *Clim. Dyn.*, doi:10.1007/s00382-008-0513-4

Lee S, and C Wang (2008) Tropical Atlantic Decadal Oscillation and Its Potential Impact on the Equatorial Atmosphere-Ocean Dynamics: A Simple Model Study, *J. Phys. Oceanogr.*, 38, 193-212

Luyten J, and Stommel H (1986) Gyres Driven by Combined Wind and Buoyancy Flux, *J. Phys. Oceanogr.*, 16, 1551-1560

Marshall JC, Nurser AJG, and Williams RG (1993) Inferring the Subduction Rate and Period over the North Atlantic, *J. Phys. Oceanogr.*, 23, 1315-1329

Marsland SJ, Haak H, Jungclaus JH, Latif M, and Röske F (2003) The Max-Planck-Institute global ocean/sea ice model with orthogonal curvilinear coordinates, *Ocean Model.* 5, 91-127

Rahmstorf S, Crucifix M, Ganopolski A, Goosse H, Kamenkovich I, Knutti R, Lohmann G, Marsh R, Mysak LA, Wang Z, and Weaver AJ (2005) Thermohaline circulation hysteresis: A model intercomparison, *Geophys. Res. Lett.*, 32, L23605, doi:10.1029/2005GL023655

Richardson PL (2007) Agulhas leakage into the Atlantic estimated with subsurface floats and surface drifters, *Deep Sea Res. Part I*, 54, 1361-1389

- Ridgway KR, and Dunn JR (2007) Observational evidence for a Southern Hemisphere oceanic supergyre, *Geophys. Res. Lett.* 34, L13612, doi:10.1029/2007GL030392
- Roeckner E, Bäuml G, Bonaventura L, Brokopf R, Esch M, Giorgetta M, Hagemann S, Kirchner I, Kornbluh L, Manzini E, Rhodin A, Schlese U, Schulzweida U, and Tompkins A (2003) The atmospheric general circulation model ECHAM 5. Part I: Model description. Tech. Rep. 349, Max-Planck-Institut für Meteorologie, Hamburg, Germany
- Schmittner A, Latif M, and Schneider B (2005) Model projections of the North Atlantic thermohaline circulation for the 21st century assessed by observations, *Geophys. Res. Lett.*, 32, doi:10.1029/2005GL024368
- Schouten MW, de Ruijter WPM, van Leeuwen PJ, and Lutjeharms JRE (2000) Translation, decay and splitting of Agulhas rings in the southeastern Atlantic Ocean, *J. Geophys. Res.*, 105, 21913-21925
- Sloyan BM, and Rintoul SR (2001) The Southern Ocean Limb of the Global Deep Overturning Circulation, *J. Phys. Oceanogr.*, 31, 143-173
- Son SW, Tandon N, Polvani L, and Waugh D (2009) Ozone hole and Southern Hemisphere climate change, *Geophys. Res. Lett.*, 36, doi:10.1029/GL038671
- Speich S, Blanke B, and Cai W (2007) Atlantic meridional overturning circulation and the Southern Hemisphere supergyre, *Geophys. Res. Lett.*, 34, L23614, doi:10.1029/2007GL031583
- Sterl A, Severijns C, Dijkstra H, Hazeleger W, van Oldenborgh GJ, van den Broeke M, Burgers G, van den Hurk B, van Leeuwen PJ, and van Velthoven P (2008) When can we expect extremely high surface temperature? *Geophys. Res. Lett.*, doi:10.1029/2008GL034071
- Stramma L, and England M (1999) On the water masses and mean circulation of the South Atlantic Ocean, *J. Geophys. Res.*, 104, 20,863-20,883
- van Sebille E, Biastoch A, van Leeuwen PJ, and de Ruijter WPM (2009) A weaker Agulhas Current leads

to more Agulhas leakage, *Geophys. Res. Lett.*, 36, L03601, doi:10.1029/2008GL036614

Vellinga M, and Wood RA (2002) Global climatic impacts of a collapse of the Atlantic thermohaline circulation, *Clim. Change*, 251-267

Weber SL, Drijfhout SS, Abe-Ouchi A, Curcifix M, Eby M, Ganopolski A, Murakami S, Otto-Bliesner B, and Peltier WR (2007) The modern and glacial overturning circulation in the Atlantic ocean in PMIP coupled model simulations, *Climate of the Past*, 3, 51-64

Weijer W, de Ruijter WPM, Sterl A, and Drijfhout SS (2002) Response of the Atlantic overturning circulation to South Atlantic sources of buoyancy, *Global and Planetary Change*, 34, 293-311

Yin J, and Stouffer RJ (2007) Comparison of the Stability of the Atlantic Thermohaline Circulation in Two Coupled Atmosphere–Ocean General Circulation Models, *J. Clim.*, 20, 4293–4315

Figure captions

Fig. 1 Maximum Atlantic meridional overturning circulation (S_v) in the control simulations (red) and in the perturbed simulations (blue). Shading indicates the spread among the simulations, thick line indicates the ensemble mean

Fig. 2 Montgomery streamlines for thermocline (a) and intermediate (b) waters in E1. The sections on panel a) are discussed in Section 4

Fig. 3 Zonally integrated layer mass transport in the Atlantic at 32°S in *Ganachaud and Wunsch* (2000; grey), *Sloyan and Rintoul* (2001; black), and E1 (blue). S stands for surface and thermocline, I for intermediate, D for deep, and B for bottom waters, as defined in the text. Positive values correspond to northward transport

Fig. 4 Change in barotropic streamfunction (HO-E2; S_v)

Fig. 5 Montgomery streamfunctions for thermocline (a) and intermediate (b) waters in E2 (red) and in HO (green)

Fig. 6 Zonally integrated layer mass transport in the Atlantic at 32°S (a) and at 25°N (b). Positive values correspond to northward transport

Fig. 7 Meridionally integrated layer mass transport in the Agulhas leakage area (23°E , $30\text{-}40^\circ\text{S}$). Positive values indicate eastward transport

Fig. 8 Zonally integrated layer mass transport at 40°S between 70-40°W in the BrC. Positive values indicate northward transport

Fig. 9 Zonally integrated layer mass transport at 2°S between 40-30°W in the NBC. Positive values indicate northward transport

Fig. 10 Zonally integrated meridional mass transport along 2°S between the Brazilian and African coasts for thermocline (a), intermediate (b) and deep (c) waters in E2 (red) and in HO (green)

Fig. 11 Mean (E2; a) and anomalous surface heatflux (HO-E2; b). Positive downward ($W \cdot m^{-2}$)

Fig. 12 Change in wind stress curl (HO-E2; in m/year). Positive values indicate reduced downwelling or increased upwelling

Fig. 13 Same as Fig. 9 for E2 (red) and E1 (blue). Positive values indicate northward transport

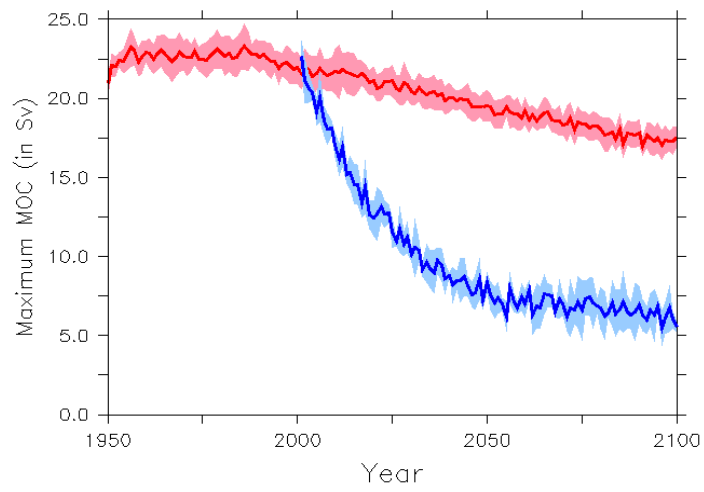


Fig. 1 Maximum Atlantic meridional overturning circulation (Sv) in the control simulations (red) and in the perturbed simulations (blue). Shading indicates the spread among the simulations, thick line indicates the ensemble mean

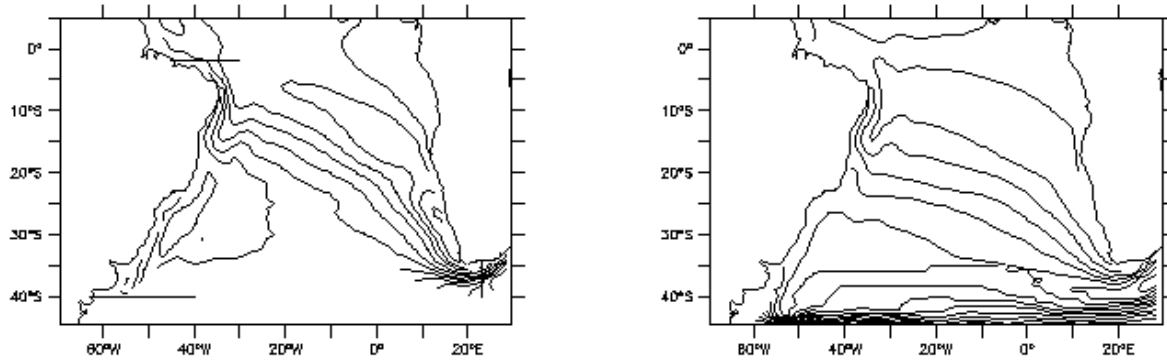


Fig. 2 Montgomery streamlines for thermocline (a) and intermediate (b) waters in E1. The sections on panel a) are discussed in Section 4

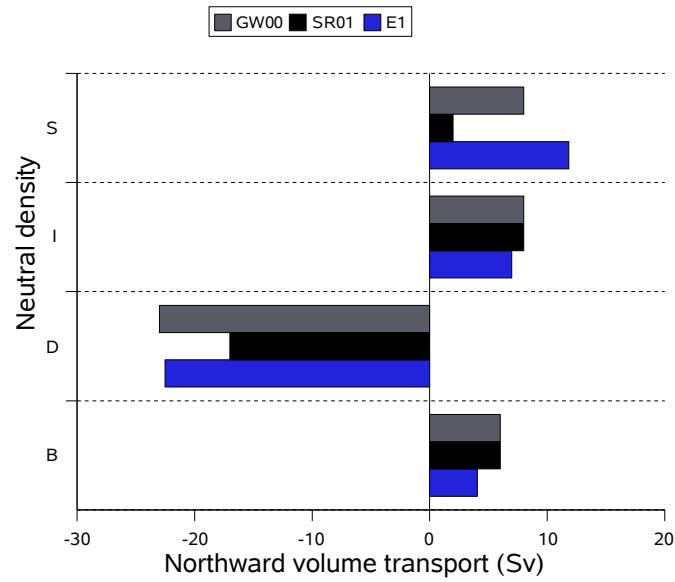


Fig. 3 Zonally integrated layer mass transport in the Atlantic at 32°S in *Ganachaud and Wunsch* (2000; grey), *Sloyan and Rintoul* (2001; black), and E1 (blue). S stands for surface and thermocline, I for intermediate, D for deep, and B for bottom waters, as defined in the text. Positive values correspond to northward transport

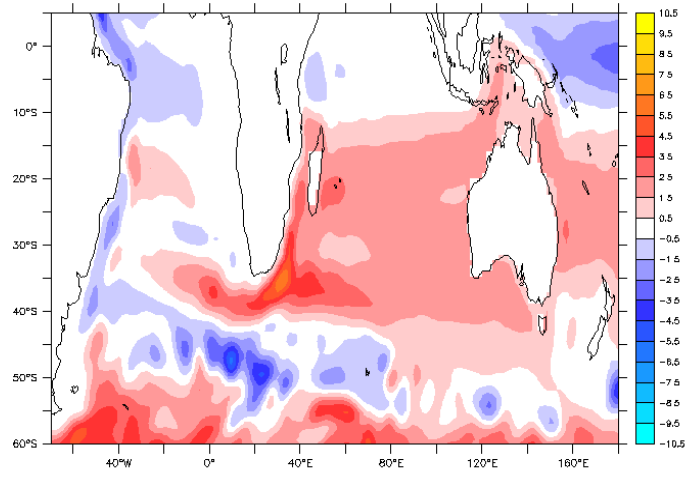


Fig. 4 Change in barotropic streamfunction (HO-E2; Sv)

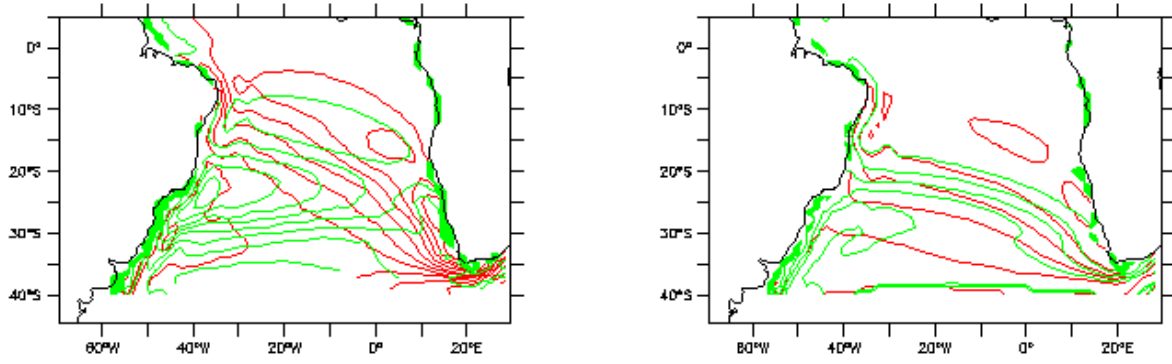


Fig. 5 Montgomery streamfunctions for thermocline (a) and intermediate (b) waters in E2 (red) and in HO (green)

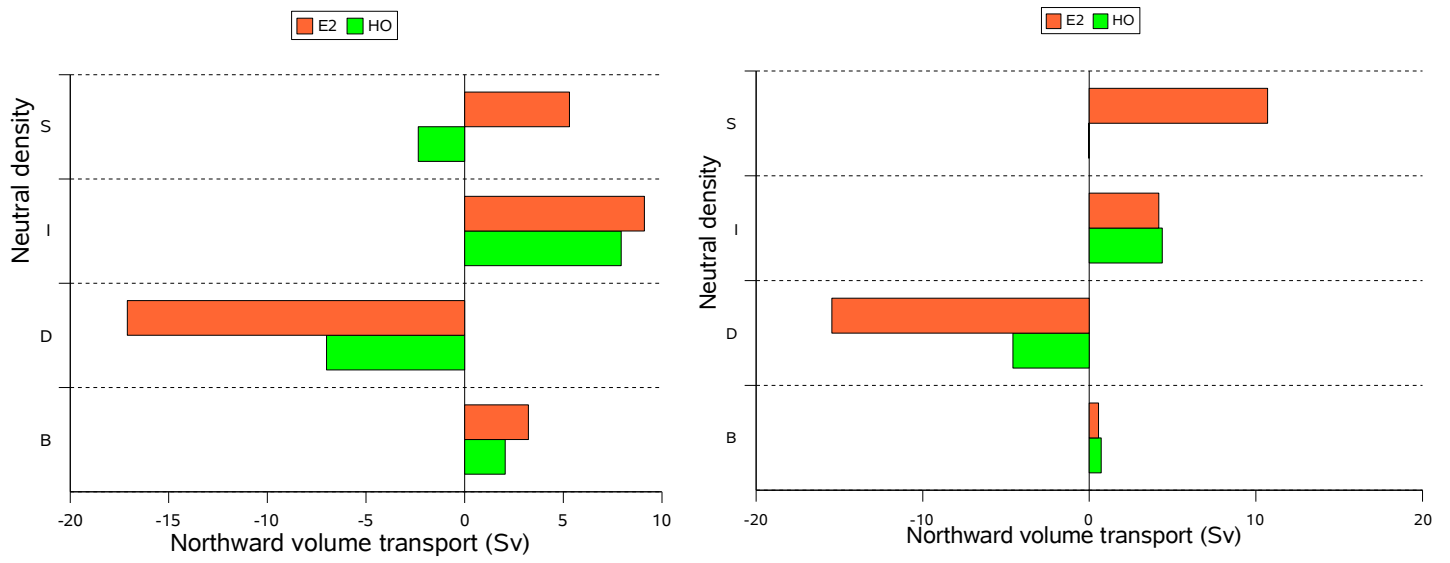


Fig. 6 Zonally integrated layer mass transport in the Atlantic at 32°S (a) and at 25°N (b). Positive values correspond to northward transport

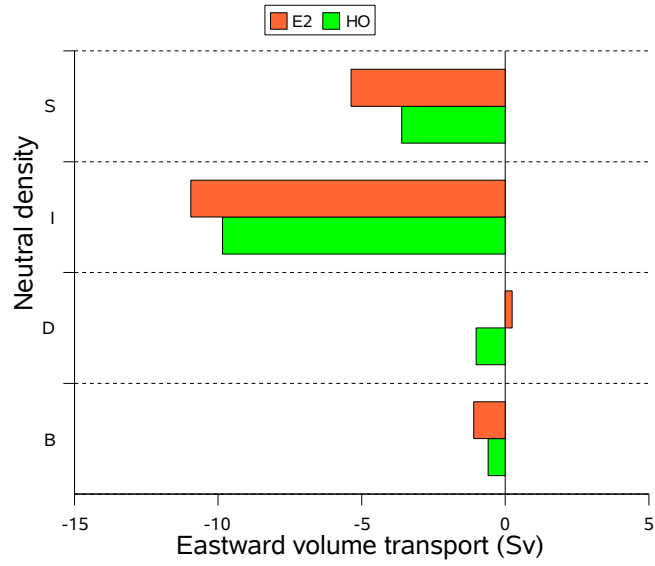


Fig. 7 Meridionally integrated layer mass transport in the Agulhas leakage area (23°E, 30-40°S). Positive values indicate eastward transport

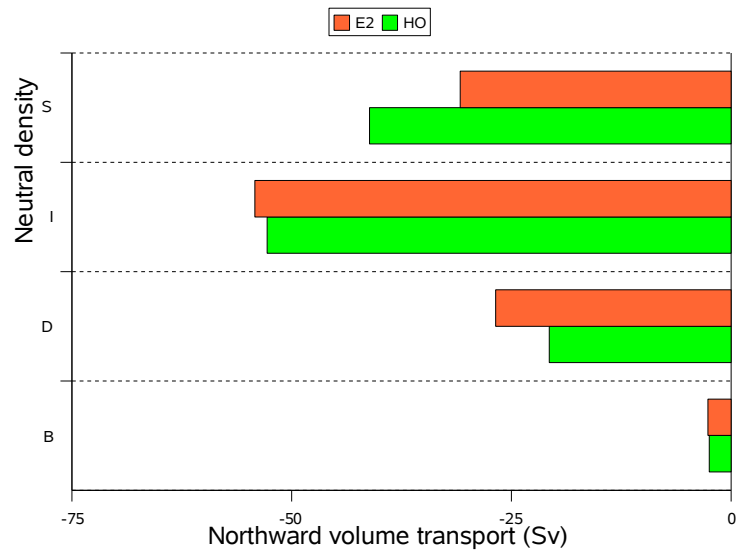


Fig. 8 Zonally integrated layer mass transport at 40°S between 70-40°W in the BrC. Positive values indicate northward transport

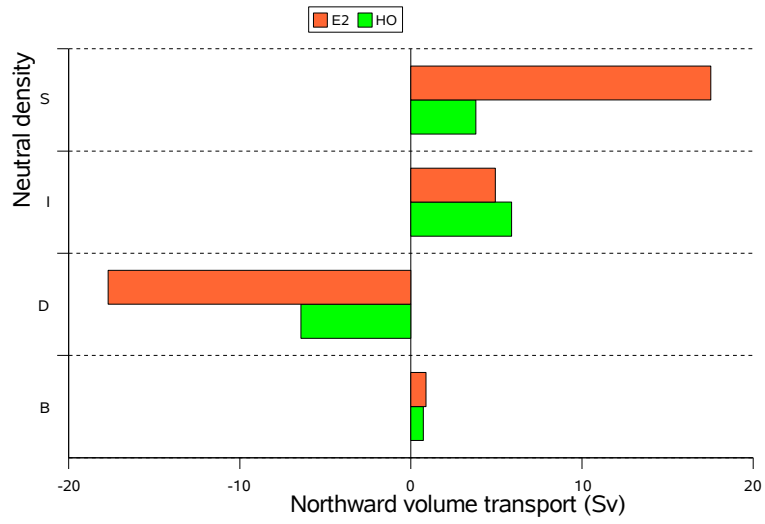


Fig. 9 Zonally integrated layer mass transport at 2°S between 40-30°W in the NBC. Positive values indicate northward transport

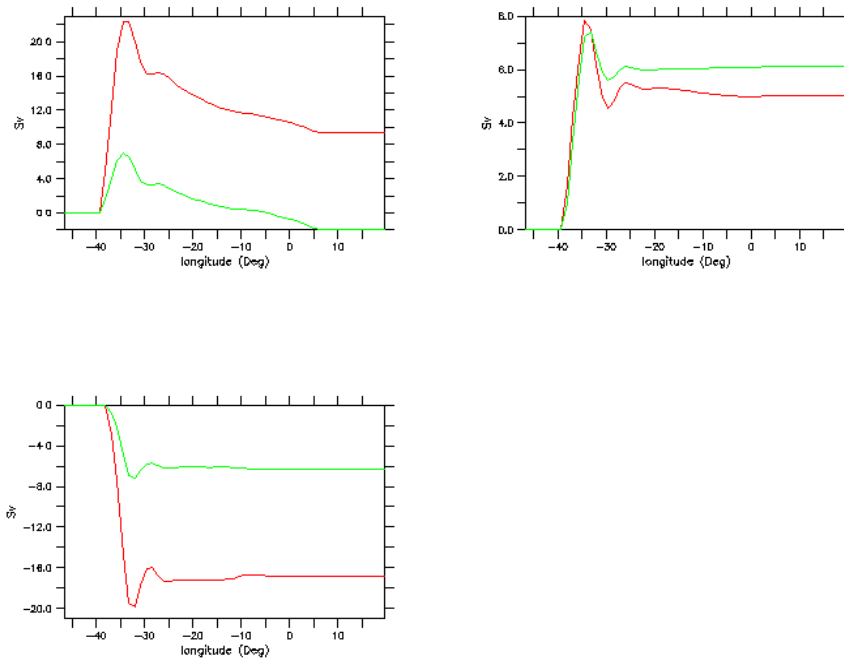


Fig. 10 Zonally integrated meridional mass transport along 2°S between the Brazilian and African coasts for thermocline (a), intermediate (b) and deep (c) waters in E2 (red) and in HO (green)

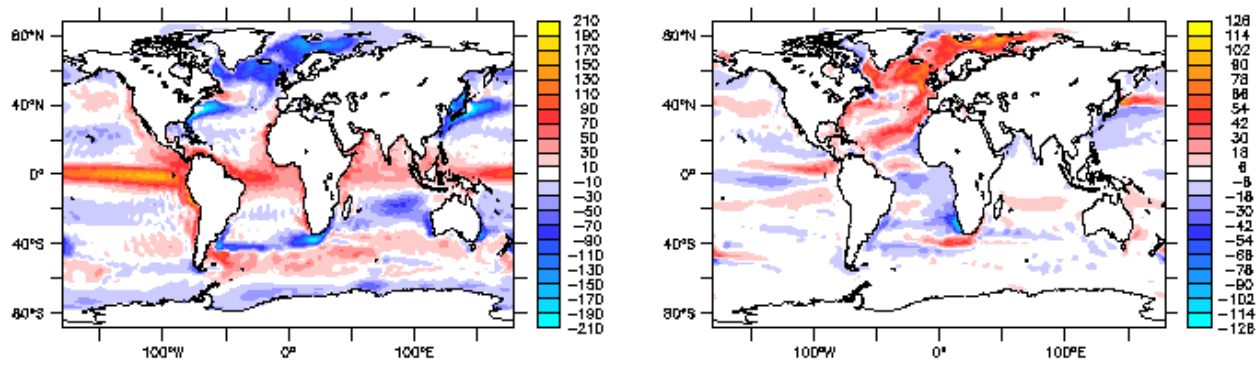


Fig. 11 Mean (E2; a) and anomalous surface heatflux (HO-E2; b). Positive downward ($W.m^{-2}$)

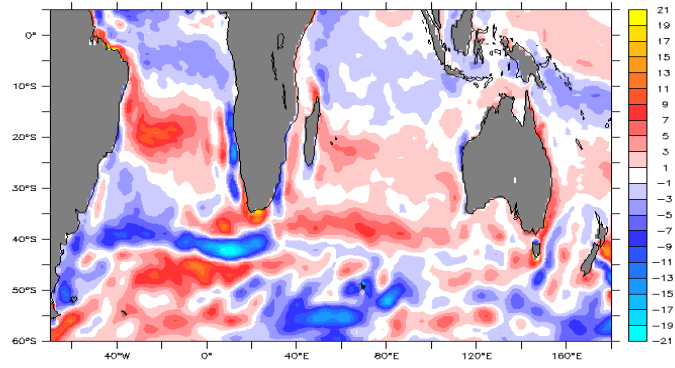


Fig. 12 Change in wind stress curl (HO-E2; in m/year). Positive values indicate reduced downwelling or increased upwelling

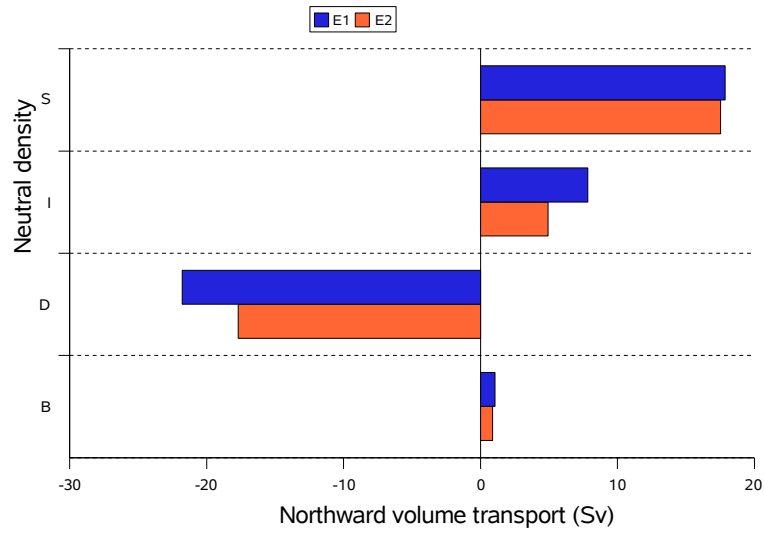


Fig. 13 Same as Fig. 9 for E2 (red) and E1 (blue). Positive values indicate northward transport